JPR Advance Access published October 13, 2015

Journal of
Plankton Research

plankt.oxfordjournals.org

J. Plankton Res. (2015) 0(0): 1–14. doi:10.1093/plankt/fbv089

Costa Rica Dome: Flux and Zinc Experiments

Phytoplankton production and grazing balances in the Costa Rica Dome

MICHAEL R. LANDRY[1]*, KAREN E. SELPH[2], MOIRA DÉCIMA[1,3], ANDRÉS GUTIÉRREZ-RODRÍGUEZ[1,4], MICHAEL R. STUKEL[5], ANDREW G. TAYLOR[1] AND ALEXIS L. PASULKA[1,6]

[1]SCRIPPS INSTITUTION OF OCEANOGRAPHY, 9500 GILMAN DR., LA JOLLA, CA 92093-0227, USA, [2]DEPARTMENT OF OCEANOGRAPHY, UNIVERSITY OF HAWAII AT MANOA, HONOLULU, HI 96822, USA, [3]NATIONAL INSTITUTE OF WATER AND ATMOSPHERIC RESEARCH (NIWA), 301 EVANS BAY PARADE, HATAITAI, WELLINGTON 6021, NEW ZEALAND, [4]CENTRE NATIONAL DE LA RECHERCHE SCIENTIFIQUE AND UNIVERSITE PIERRE ET MARIE CURIE, STATION BIOLOGIQUE, ROSCOFF 29680, FRANCE, [5]EARTH, OCEAN AND ATMOSPHERIC SCIENCE, FLORIDA STATE UNIVERSITY, TALLAHASSEE, FL 32306, USA AND [6]GEOLOGICAL AND PLANETARY SCIENCES, CALIFORNIA INSTITUTE OF TECHNOLOGY, PASADENA, CA 91125, USA

*CORRESPONDING AUTHOR: mlandry@ucsd.edu

Received April 11, 2015; accepted September 15, 2015

Corresponding editor: John Dolan

We investigated phytoplankton production rates and grazing fates in the Costa Rica Dome (CRD) during summer 2010 based on dilution depth profiles analyzed by flow cytometry and pigments and mesozooplankton grazing assessed by gut fluorescence. Three community production estimates, from ^{14}C uptake (1025 ± 113 mg C m^{-2} day^{-1}) and from dilution experiments analyzed for total Chl*a* (990 ± 106 mg C m^{-2} day^{-1}) and flow cytometry populations (862 ± 71 mg C m^{-2} day^{-1}), exceeded regional ship-based values by 2–3-fold. Picophytoplankton accounted for 56% of community biomass and 39% of production. Production profiles extended deeper for *Prochlorococcus* (PRO) and picoeukaryotes than for *Synechococcus* (SYN) and larger eukaryotes, but 93% of total production occurred above 40 m. Microzooplankton consumed all PRO and SYN growth and two-third of total production. Positive net growth of larger eukaryotes in the upper 40 m was balanced by independently measured consumption by mesozooplankton. Among larger eukaryotes, diatoms contributed ~3% to production. On the basis of this analysis, the CRD region is characterized by high production and grazing turnover, comparable with or higher than estimates for the eastern equatorial Pacific. The region nonetheless displays characteristics atypical of high productivity, such as picophytoplankton dominance and suppressed diatom roles.

KEYWORDS: productivity; grazing; plankton community

available online at www.plankt.oxfordjournals.org

INTRODUCTION

The Eastern Tropical Pacific (ETP) is a large region of complex currents and contrasting ecosystems that extends from ~20°N to 20°S off the west coasts of North and South America to ~140°W along the equator, nearly half way across the Pacific Ocean. Within the ETP, several productive areas, like the Peruvian coastal upwelling system and the eastern equatorial cold-tongue region, are well known and richly characterized (Chavez *et al.*, 1996; Fiedler and Talley, 2006). In contrast, other potential production centers are recognized but poorly understood. The Costa Rica Dome (CRD), residing several hundred kilometers off the coast of Central America ~9°N, 90°W, is one such system. Open-ocean upwelling develops seasonally at the CRD associated with the western shoaling of the 10°N thermocline ridge (Fiedler, 2002). In mid-summer satellite images, the CRD is often the most prominent open-ocean area of elevated chlorophyll in the northern ETP.

In a recent review of ETP productivity, Pennington *et al.* (Pennington *et al.*, 2006) found that the primary production was well explained and constrained on a regional basis by variability in nutrient delivery related to thermocline depth. Within subregions of the ETP, however, there were many discrepancies between ship measurements and model estimates of production rates. In the Costa Rica Dome, for example, the few modern field estimates of depth-integrated production rates ($n = 22$) average ~3-fold less than model predictions of productivity, and they are about half of the ship-measured rates for production in the eastern equatorial upwelling area. Because trophic studies in the dome region are rare, it is difficult to know whether the characterization of the CRD as the only modestly productive area relative to the better studied equatorial upwelling area is valid, and, if so, what that difference might mean for carbon flows and cycling within the euphotic zone, the potential efficiencies of production transfer to higher trophic levels and export and the contributions of phytoplankton functional groups to those fluxes.

Standing stock measurements and process-rate experiments from the CRD Flux and Zinc Experiments cruise in June–July 2010 allow for the first time a coherent analysis of production rates and grazing fates in the CRD region. As these data will illustrate, the summertime CRD is, in fact, as productive as or more productive than the eastern equatorial upwelling region while nonetheless retaining distinctive features associated with low production, such as high picophytoplankton dominance and suppressed roles for diatoms.

METHOD

We measured plankton community standing stocks and process rates in the Costa Rica Dome during the CRD FLUx and Zinc Experiments (FLUZiE) project on *R/V Melville* cruise MV1008 (22 June–25 July 2010). Five quasi-Lagrangian experiments, termed 'cycles', were conducted on the cruise, each organized as 3- to 4-day sets of daily-repeated sampling and incubation activities following the path of a satellite-tracked drifter with a 3-m drogue centered at 15 m (Landry *et al.*, 2009).

For each daily experiment, we collected seawater on an early-morning hydrocast (~02:00 local time) at eight depths in the euphotic zone: 2, 12, 20 and generally 30 m, plus four deeper depths to 80–100 m, which varied depending on the fluorescence profile. Water samples from each depth were used to assess the abundance and biomass of phytoplankton (Taylor *et al.*, 2015) and heterotrophic protists (Freibott *et al.*, this issue) and to determine the rates of phytoplankton growth, microzooplankton grazing and ^{14}C primary production (Selph *et al.*, 2015). At mid-day (1000–1100) and mid-night (2200–2300), we also towed a plankton net obliquely through the euphotic zone to determine mesozooplankton biomass and gut-fluorescence estimates of grazing (Décima *et al.*, 2015). The studies cited above comprise the primary sources of biomass and rate data for the present analysis and provide more detailed accounts of the methods, results and interpretations.

Experimental setup

Water for standing stock samples and incubations came from the same early-morning hydrocasts taken within ~100 m of the drift array from Niskin bottles on a CTD rosette. Samples for initial concentrations of pigments, shipboard flow cytometric counting and enumeration of plankton populations by microscopy were filled directly from the Niskin bottles via acid-washed silicone tubing. For ^{14}C-uptake (community net production), we filled two light bottles and one dark bottle (250 mL, acid-cleaned polycarbonate) with water from each depth and inoculated them with 100 μL of ^{14}C $NaHCO_3$ stock. For dilution experiments, we followed the two-treatment dilution approach (Landry *et al.*, 2008, 2011b), preparing, for each sampling depth, a pair of polycarbonate bottles (2.7 L) containing unfiltered seawater (100%) and a mixture of ~34% whole seawater and 0.1-μm filtered seawater from that depth. Seawater was filtered directly from the Niskin bottles using a peristaltic pump, silicone tubing and an in-line Suporcap filter capsule that had previously been acid-washed (3.7% trace-metal grade HCl; Milli-Q and seawater rinses). Dilution treatment bottles first received measured volumes of filtered water, and were then gently filled with unscreened water from the Niskin bottles. After preparation, each bottle was subsampled for flow cytometric analysis (1 mL) for initial

concentrations and to confirm volumetric dilutions for other variables.

^{14}C-uptake and dilution bottles were tightly capped, placed into mesh bags and clipped onto attached rings at the depth of collection on a line below the drift array float. The preparation process, from CTD arrival on deck to array deployment, was generally completed within 2 h and always prior to local sunrise. Experiments on adjacent days were set up first on deck. Then, the array was hand-recovered, the net bags switched and the array redeployed in 15–20 min. Upon recovery, ^{14}C-uptake samples were filtered onto 25-mm Whatman glass-fiber filters (GF/F grade) and placed in scintillation vials. One mL of 10% HCl was added to each sample, and the acidified samples were allowed to sit, without a cap, at room temperature for at least 3 h before Ecolume cocktail (10 mL) was added. The vials were then capped and mixed before being counted on a Beckman 6100LC liquid scintillation counter at 1.0% counting precision. Upon array recovery, all dilution bottles were immediately subsampled for final assessments of phytoplankton composition and biomass by flow cytometry, high-pressure liquid chromatography (HPLC) pigments and epifluorescence microscopy.

Microplankton community analyses

We assessed abundances, biomass and composition of the microbial community using a combination of laboratory and shipboard flow cytometry (FCM), taxon-specific accessory pigments (HPLC) and epifluorescence microscopy (EPI) (Taylor *et al.*, 2015). Population abundances of picophytoplankton [*Prochlorococcus* (PRO), *Synechococcus* (SYN) and phototrophic eukaryotes (P-Euk)] were determined from 1-mL FCM samples, which were preserved with 0.5% paraformaldehyde (v/v, final concentration), frozen in liquid nitrogen and stored at −80°C until analysis. In the laboratory, the samples were thawed and stained with Hoechst 33342 (1 μg mL^{-1}, v/v, final concentration) at room temperature in the dark for 1 h (Monger and Landry, 1993). Aliquots (100 μL) were analyzed using a Beckman Coulter EPICS Altra flow cytometer with a Harvard Apparatus syringe pump for volumetric sample delivery. Simultaneous (co-linear) excitation of the plankton was provided by two water-cooled 5-W argon ion lasers, tuned to 488 nm (1 W) and the UV range (200 mW). Populations were distinguished based on chlorophyll *a* (red fluorescence, 680 nm), phycoerythrin (orange fluorescence, 575 nm), DNA (blue fluorescence, 450 nm) and forward and 90° side-scatter signatures. Calibration beads (0.5- and 1.0-μm yellow-green beads and 0.5-μm UV beads) were used as fluorescence standards. Listmode files were processed using the FlowJo software.

Shipboard FCM was done within 1–2 h of collection on unpreserved samples kept on ice in the dark until analysis. The shipboard cytometer was a Beckman Coulter XL with a 15-mW, 488-nm argon ion laser with an Orion syringe pump that delivered 2.2-mL samples at a rate of 0.44 mL min^{-1}. Listmode files of cell fluorescence and light scatter properties were acquired with Expo32 software and analyzed with the FlowJo software. Fluorescence signals were normalized to 1.0-μm yellow-green beads.

Concentrations of chlorophyll and carotenoid pigments were determined using HPLC on 1.6–2.2-L samples filtered onto Whatman GF/F filters, stored in liquid nitrogen and extracted in acetone. Using canthaxanthin as an internal standard, we analyzed samples on an Agilent 1100 HPLC system with a Waters Symmetry C8 column (3.5-μm particle size, 4.6 × 150 mm, silica, reverse phase). Pigments were eluted using two solvent gradients following the method of Goericke (Goericke, 2002). Fluorometric determinations of Chl*a* were also made on shipboard for 250-mL samples, extracted in 90% acetone (−20°C, dark) and read on a Turner Designs TD-700 fluorometer using standard equations calibrated with pure Chl*a*.

For EPI analyses of single-celled eukaryotes (protists), seawater samples (500 mL) were preserved with 260 μL of alkaline Lugol's solution, 10 mL of buffered formalin and 500 μL of sodium thiosulfate, gently mixing between additions (Sherr and Sherr, 1993). After 1 h of fixation, the preserved samples were stained with 1 mL of proflavin (0.33% w/v) and 1 mL of DAPI (0.01 mg mL^{-1}) prior to filtering. Subsamples of 50 mL were filtered onto 25-mm, black, 0.8-μm pore polycarbonate filters to enumerate smaller cells at ×630 magnification. The remaining sample (450 mL) was filtered onto a 25-mm, black, 8.0-μm pore polycarbonate filter to enumerate larger cells at ×200 magnification. Each filter was mounted onto a glass slide using Type DF immersion oil and frozen at −80°C until analysis. The slides were imaged and digitized using an automated Zeiss Axiovert 200 M inverted epifluorescence microscope, with a Zeiss AxioCam HRc color CCD digital camera (Taylor *et al.*, 2015).

We used ImagePro software to analyze cells larger than 1.5 μm in length, with each identified cell assigned to one of seven functional groups: diatoms, autotrophic dinoflagellates (A-Dino), prymnesiophytes (Prym), cryptophytes (Crypto), autotrophic flagellates (A-Flag), heterotrophic dinoflagellates (H-Dino) and heterotrophic flagellates (H-Flag), with A- and H-Flag categories containing all cells that could not be placed into taxon-defined groups. Autotrophic cells were identified by the presence of Chl*a* (red autofluorescence under blue-light

excitation), generally packaged in defined chloroplasts. Obvious heterotrophic cells with recently consumed prey were manually excluded. Cell biovolumes (BV; μm^3) were determined from length (L) and width (W) measurements using the formula for a prolate sphere ($BV = 0.524 \times L \times W^2$). Carbon (C; pg $cell^{-1}$) biomass of eukaryotic cells was computed from BV using the following equations: $C = 0.216 \times BV^{0.939}$ for non-diatoms, and $C = 0.288 \times BV^{0.811}$ for diatoms (Menden-Deuer and Lessard, 2000).

Autotroph carbon estimates include FCM-analyzed populations in addition to microscopy. Abundance estimates of PRO and SYN from laboratory-based FCM analyses were converted to carbon biomass using carbon conversions for surface populations (32 and 101 fg C $cell^{-1}$ for PRO and SYN, respectively; Garrison *et al.*, 2000; Brown *et al.*, 2008), adjusted for BV changes with depth using bead-normalized forward-angle light scattering ($FALS^{0.55}$) as a scaling factor (Binder *et al.*, 1996; Landry *et al.*, 2003). We used the difference between total cell counts of <5-μm cells from EPI and P-Euks enumerated by FCM laboratory analyses to estimate the <1.5-μm cells missed by microscopy. Assuming that the missing cells were between 0.8 and 1.5 μm, a mean biomass of 192 fg C $cell^{-1}$ was computed (Menden-Deuer and Lessard, 2000), and the resulting biomass was added to the EPI estimate for 1.5–2 μm cells to get total picoeukaryote carbon.

Rate determinations

From the two-bottle dilution experiments, we determined rate profiles for phytoplankton growth (μ, day^{-1}) and microzooplankton grazing (m, day^{-1}) from each pair of incubated bottles and for each FCM or pigment-associated population of interest. Assuming a linear decline in grazing mortality with dilution, as confirmed by full dilution experiments conducted on this cruise (Selph *et al.*, 2015), the net rate of change (k) of a measured parameter is $k = \mu - m$ in the undiluted bottles and $k_d = \mu - 0.34 \times m$ in diluted bottles, where 0.34 is the fraction of natural grazer density in the dilute treatment. The following two equations are solved for the two unknowns, μ and m:

$$m = \frac{k_d - k}{1 - 0.34} \quad \text{and} \quad \mu = k + m.$$

Population-specific rates were determined directly from the initial and final abundances of FCM-measured populations. PRO abundances were reliably determined only in the frozen small-volume samples. SYN abundances were similar in both laboratory FCM and shipboard live analyses, but the shipboard analyses were used for rate determinations because those subsample volumes analyzed were >20× greater. Similarly, the larger volume, live-shipboard analyses were better suited for rate determinations of eukaryotic cells, which were separated into small (pico) and larger (micro) size classes but unresolved with regard to taxonomic group. Group-specific rate estimates for eukaryotic algae were determined from HPLC pigment values corrected for changes in cellular pigment content over the 24-h incubations using bead-normalized red fluorescence (Landry *et al.*, 2011b; Selph *et al.*, 2015). We used normalized red-fluorescence changes for SYN and eukaryotes, scaled to the relative contributions of each to their combined biomass, to derive corrections for monovinyl Chl*a* (MVChl*a*). Corrections for total chlorophyll *a* (TChl*a*) were determined by the red-fluorescence corrections for combined PRO, SYN and eukaryotes, and their proportional contributions to TChl*a*. Depth profiles of pigment corrections for eukaryotic phytoplankton (as well as for Chl*a*) were statistically indistinguishable for the four cycles (2–5) for which we had data for comparison (Selph *et al.*, 2015). We consequently applied the same mean depth corrections to all HPLC pigments for the Cycle 2–5 experiments.

Carbon-based estimates of phytoplankton community production (PP) and microzooplankton grazing (PG) were calculated using growth (μ) and grazing (m) rates based on TChl*a* from dilution experiments and the following equations (Landry *et al.*, 2000):

$$PP = \frac{\mu \times C_o(e^{(\mu - m)t} - 1)}{(\mu - m)t} \quad \text{and}$$

$$PG = \frac{m \times C_o(e^{(\mu - m)t} - 1)}{(\mu - m)t}$$

where C_o is initial autotrophic biomass (mg C m^{-3}) and t = time (1 day). Similarly, taxon-specific estimates of carbon production and grazing were calculated for components of the community where parameter estimates of μ and m could be reasonably associated with a C-based estimate of standing stock. For example, production rates of PRO, SYN, diatoms and prymnesiophytes were determined from initial (C_o) biomass estimates for each group and rate assessments from FCM cell counts (PRO and SYN), fucoxanthin (FUCO) and 19′-hexanoyloxyfucoxanthin (HEX), respectively. Carbon-based rates for the remaining taxa (= Other Eukaryotes) could not be reliably distinguished, either because group-specific biomass could not be determined from microscope analyses (pelagophytes and prasinophytes) or because group-associated accessory pigments were too low for reliable rate assessments. This was notably a problem for peridinin (PER), the accessory pigment found in some, but not all,

dinoflagellates. For the Other Eukaryote group, we used the remaining biomass total (dinoflagellates and unidentified to group) along with rate estimates based on the sum of other group-specific accessory pigments to compute carbon production and grazing estimates. All production rate calculations were made for each incubation light depth at each station separately and then vertically integrated.

Mesozooplankton grazing estimates

We used a 1-m ring net with 202-μm Nitex mesh for mesozooplankton collections (Décima *et al.*, 2015). The net was towed obliquely for 20 min at a ship speed of ~2 km h^{-1}, with a General Oceanics flowmeter recording volume filtered and a Vemco depth logger recording tow depth and duration. On recovery, cod end contents were anesthetized with carbonated water to prevent gut evacuation (Kleppel and Pieper, 1984), then size-fractioned (0.2–0.5, 0.5–1, 1–2, 2–5 and >5 mm), concentrated onto 200-μm Nitex filters and frozen in liquid nitrogen for later processing. Except for the largest size fraction (>5 mm analyzed whole), all other sizes were subsampled and analyzed in duplicate. Typically 1/8 (0.2, 0.5 and 1 mm size classes) or 1/2 (2 mm size class) of the filter was subsampled with a razor blade, added to a test tube with 7 mL of 90% acetone and sonicated with a tissue homogenizer. Test tubes were kept on ice before and after this process, and pigment extraction was done in the dark at −20°C for 2–4 h before centrifuging at 3000 g for 5 min to remove particles. Chl*a* and phaeopigments (Phaeo) were analyzed using a 10 AU Turner fluorometer, before and after acidification (Strickland and Parsons, 1972). Euphotic zone estimates of gut Phaeo concentration (GPC, mg Phaeo m^{-2}) were computed from sample concentration, fraction of net tow analyzed, tow depth and volume of water filtered. These were used uncorrected for conversion to non-fluorescent products (Durbin and Campbell, 2007). In subsequent calculations, we used GPC estimates from the paired day–night tows at each station to average out diel biases in grazing activity and vertical migration. For a few stations where paired tows were not available, we estimated the missing tows using mean day:night ratios at the other stations.

Daily instantaneous rates of phytoplankton mortality (M, day^{-1}) from mesozooplankton grazing were computed as

$$M = \mathrm{GPC} \cdot 24 \cdot K \cdot \mathrm{Chl}_z{}^{-1}$$

where K (h^{-1}) is the gut evacuation rate constant of 2.1 h^{-1} derived experimentally at a similar temperature from shipboard gut experiments in the equatorial Pacific (Zhang *et al.*, 1995) and Chl_z is the depth-integrated concentration of Chl*a* in the euphotic zone (mg Chl*a* m^{-2}) (Décima *et al.*, 2011).

RESULTS

Production and grazing profiles

The present analysis provides three complementary approaches for resolving depth profiles of PP (^{14}C-uptake, estimates from community C biomass and TChl*a* growth rates from dilution experiments, and estimates from the combined contributions of FCM-based populations to production) (Figs 1 and 2). The latter two approaches also give independent assessments of carbon consumption by microzooplankton.

Depth profiles for the FCM populations display different features in the CRD (Fig. 1). The photosynthetic bacteria, *Prochlorococcus* (PRO) and *Synechococcus* (SYN), for instance, show remarkable coherence of production and grazing, on average, throughout the depth profiles. Near-surface rates for SYN are 7–8 times higher than for PRO, but SYN productivity and grazing drop off sharply in the upper 20 m, whereas PRO rates decline by less than 50% over the upper 40 m. Though less dramatic, the relative activity of P-Euks extends deeper in the euphotic zone than the mean profile for larger (nano-/microsized) eukaryotes. The eukaryotes, more notably the larger algae, also show substantial separation between production and grazing profiles that is not seen for the photosynthetic bacteria. Below 40 m, production and grazing are reasonably in balance for all populations. Above 40 m, there is a production surplus attributable to eukaryotic algae that escape microzooplankton grazing. Rate profiles for FCM populations further indicate that the production of larger eukaryotes exceeds the combined contributions of pico-sized populations (PRO, SYN and P-Euks) at all depths. However, most carbon consumed by microzooplankton is attributable to picophytoplankton.

Figure 2 compares the production and grazing profiles for the sum of FCM populations (Fig. 1) to rate profiles from shipboard fluorometric analyses of TChl*a* (Fluor Chl*a*) from the same experiments and to mean profiles of phytoplankton carbon biomass and ^{14}C-primary production incubated under the same *in situ* conditions. All profiles are averaged for the 13 experiments (Exps. 4–16; Table I) for which we have full data on all variables. While the FCM and TChl*a* profiles show similar magnitudes and features, the pigment analyses give somewhat higher production values and lower grazing estimates, and therefore larger net production surplus in the euphotic zone that is not consumed by microzooplankton. However, neither the FCM- nor the pigment-derived dilution results reproduce exactly the carbon production profiles from ^{14}C-bicarbonate

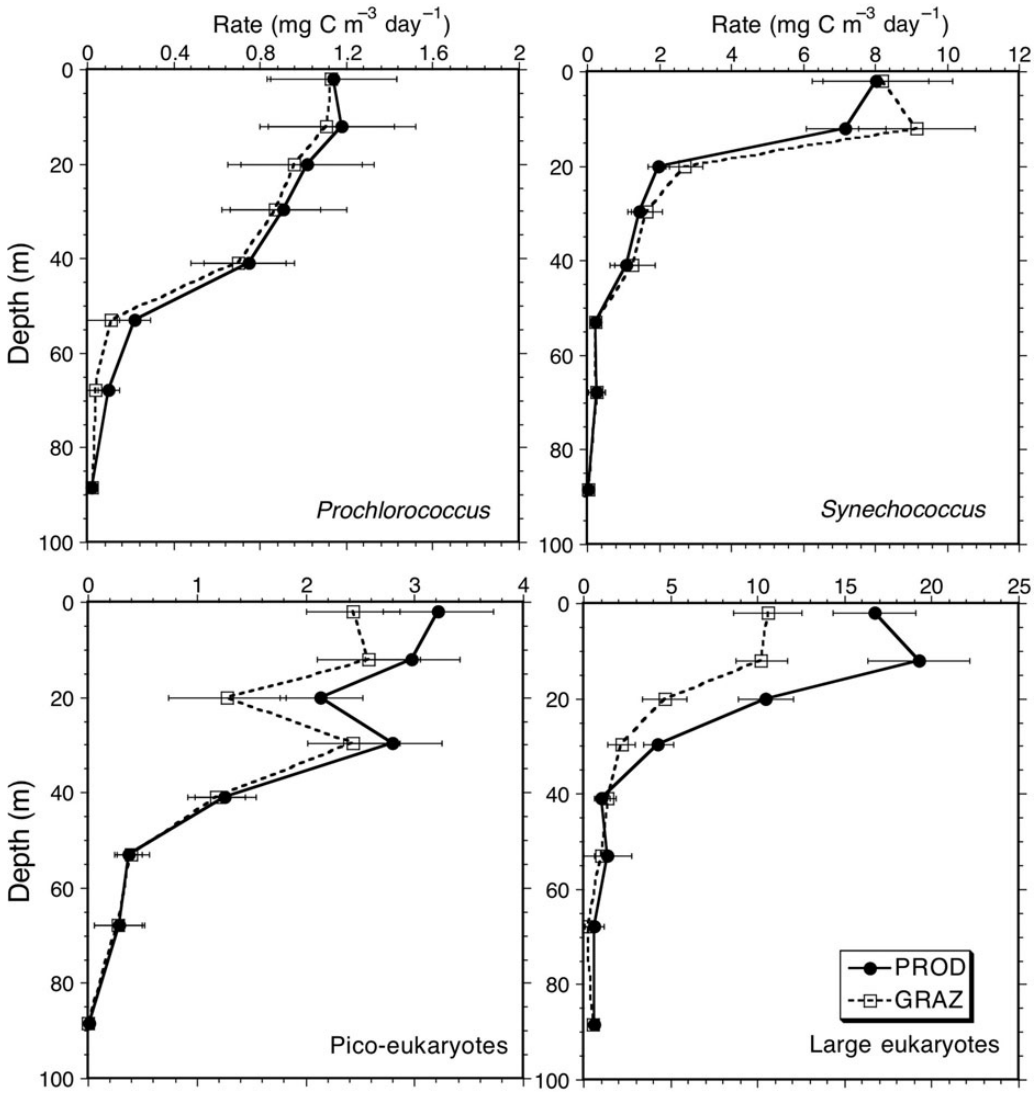

Fig. 1. Depth profiles for production (PROD) and microzooplankton grazing (GRAZ) from 24-h *in situ* dilution incubations in the Costa Rica Dome area, analyzed for flow cytometrically determined populations (*Prochlorococcus*, *Synechococcus*, picoeukaryotes and large eukaryotes). Error bars are standard errors of mean estimates.

uptake. The biggest discrepancy is the higher production for the shallowest incubated samples (2 m) in the ^{14}C profile, which exceeds 50 mg C m^{-3} day^{-1} on average. Dilution profiles suggest, in contrast, that production is lower (~30 mg C m^{-3} day^{-1}) and more uniform over the upper 12 m. Deeper in the euphotic zone, 30 m and below, dilution estimates exceed those from ^{14}C (Fig. 2). Nonetheless, depth-integrated carbon production values are highest for ^{14}C [1025 ± 113 mg C m^{-2} day^{-1}; mean ± standard error (SE)], slightly lower for TChl*a* (990 ± 106 mg C m^{-2} day^{-1}) and lowest overall for the composite FCM profiles (859 ± 73 mg C m^{-2} day^{-1}). Despite these differences, however, all values are 2–3-fold higher than previous mean field production estimates for the CRD region (Pennington *et al.*, 2006).

Production and grazing balance

In Table I, we evaluate production and grazing balances for individual experiments by combining TChl*a* estimates of phytoplankton growth and microzooplankton grazing rates with mesozooplankton estimates of grazing impact based on gut pigment measurements (Décima *et al.*, 2015). Each of these daily experiments involved a 24-h *in situ* rate profile of dilution experiments to determine mean instantaneous rates of phytoplankton growth and

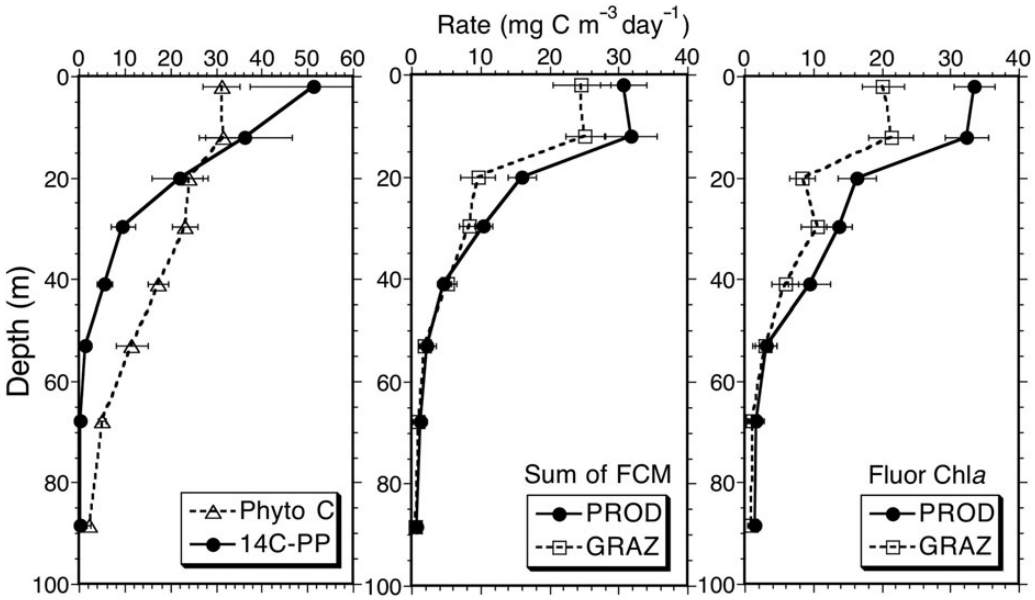

Fig. 2. Depth profiles for total phytoplankton carbon (Phyto C), primary production by ^{14}C-bicarbonate uptake (14C-PP) and phytoplankton production (PROD) and microzooplankton grazing (GRAZ) from dilution experiments in the Costa Rica Dome area (July 2010). Carbon-based rate estimates for the phytoplankton community are done two ways from dilution experiments: the sum of flow cytometrically determined populations (sum of FCM) and from fluorometrically measured chlorophyll *a* (Fluor Chl*a*). All experiments were incubated *in situ* for 24 h at the depth of sample collection. Error bars are standard errors of mean estimates.

Table I: Phytoplankton growth–grazing balances for in situ incubation experiments in the Costa Rica Dome (June–July 2010)

Exp.	Date	Lat. (°N)	Lon. (°W)	μ (day^{-1})	*m* (day^{-1})	*M* (day^{-1})	Net (day^{-1})
1	24 June	9.72	87.00	0.16	0.08	0.19	−0.11
2	25 June	9.66	86.87	0.66	0.68	0.25	−0.28
3	26 June	9.60	86.83	0.09	0.09	0.11	−0.11
4	4 July	9.04	90.56	0.40	0.28	0.09	0.03
5	5 July	9.04	90.50	0.42	0.45	0.09	−0.12
6	6 July	8.95	90.49	0.47	0.31	0.13	0.03
7	7 July	8.95	90.55	0.21	0.40	0.14	−0.33
8	9 July	10.42	92.92	0.79	0.34	0.68	−0.23
9	10 July	10.17	92.95	0.45	0.27	0.46	−0.28
10	11 July	10.14	92.98	0.76	0.45	1.82	−1.51
11	12 July	9.98	92.92	0.41	0.48	0.38	−0.45
12	15 July	8.54	90.40	0.71	0.33	0.31	0.07
13	16 July	8.53	90.32	0.92	0.31	0.39	0.22
14	17 July	8.50	90.38	0.42	0.20	0.12	0.12
15	18 July	8.58	90.18	0.99	0.55	0.15	0.29
16	20 July	8.88	88.46	1.05	0.45	0.64	0.08
17	21 July	9.09	88.20	0.57	0.22	0.70	−0.35
18	22 July	9.15	87.89	0.55	0.18	1.26	−0.89
19	23 July	9.31	87.71	0.63	0.30	0.35	−0.02
	MEAN			0.56	0.34	0.43	−0.20
	SE			0.06	0.03	0.10	0.10

μ, phytoplankton growth rate; *m*, mortality rate due to microzooplankton grazing; *M*, mortality rate due to mesozooplankton grazing; Net = μ − (*m* + *M*). All rates (day^{-1}) are depth-integrated averages for the euphotic zone.

microherbivory integrated over the euphotic zone, as well as mid-day and mid-night net tows for mesozooplankton, from which we determined day–night averages of grazing impact for the euphotic zone based on gut pigments. Since only a nighttime tow was done for experiments 14, 16 and 18, the resulting estimates were multiplied by 0.82, the average ratio of mean day–night values to nighttime values for the other experiments.

While individual experiments differ substantially with regard to there being a net production surplus (+) or deficit (−) of phytoplankton growth, it is clear that estimates of mesozooplankton grazing are more than sufficient to account for the differences seen in production and grazing profiles from the dilution incubations (Fig. 2). In fact, our analysis indicates that there is more combined grazing by micro- and mesoherbivores than production to support it. As will be discussed later, it could be that inadvertent contamination of the net tow samples with pigmented debris led to overestimates of mesozooplankton grazing in some cases, thus contributing to the imbalance. Here, however, we accept the estimates at face value and incorporate them into the community carbon-based analysis that follows below (Table II). We note nonetheless that six of the experiments where grazing exceeded growth in Table I (Exps. 1–3 and 17–19) did not have the full complement of biomass and rate data, and therefore are excluded from the subsequent analysis.

Production rates and fates

Phytoplankton community biomass during the period of our experiments averaged 1390 ± 133 mg C m^{-2} (mean ± SE), of which 39% was attributable to photosynthetic bacteria (157 ± 21 and 392 ± 68 mg C m^{-2} for PRO and SYN, respectively), 56% to picophytoplankton generally (including PRO, SYN and 230 ± 14 mg C m^{-2} for picoeukaryotes) and a very small percentage (~1%; 15 ± 3 mg C m^{-2}) to diatoms (Table II). Among distinguishable eukaryotes in microscope analyses (Taylor *et al.*, 2015), dinoflagellates contributed most to phytoplankton biomass (22%; 302 ± 51 mg C m^{-2}), and prymnesiophytes were also significant (~7%; 103 ± 7 mg C m^{-2}). Unfortunately, low PER concentrations in many of the experiments precluded using that pigment as a diagnostic indicator for dinoflagellates. The Other Eukaryote category thus represents a mixed category of eukaryotes, including dinoflagellates, pelagophytes, prasinophytes and others not clearly recognizable as diatoms or prymnesiophytes.

For the phytoplankton community as a whole, the production estimate of 990 ± 106 mg C m^{-2} day^{-1} derived from TChl*a*-based rates is balanced, on average, by losses to grazing, of which 66% (645 ± 62 mg C m^{-2} day^{-1}) is attributable to microzooplankton herbivory and 35% (349 ± 64 mg C m^{-2} day^{-1}) grazed by mesozooplankton (Table II). Together, the two independently measured grazing components exceed production slightly (+1%), but the offset is well within measurement error. From the same profile, estimates based on fluorometric TChl*a*, production and grazing integrations to 40 m account for 93% of the rates for the full euphotic zone. Thus, the lower euphotic zone, where accurate determinations are more difficult due to lower standing stocks and growth rates, can be reasonably ignored for analyses of group-specific contributions. Comparative assessments of 0–40 m production rates for the same experiments based on TChl*a*

Table II: Community and taxon-specific estimates of phytoplankton biomass, production and grazing in the Costa Rica Dome, July 2010

Category	Biomass (mg C m^{-2})	Production (mg C m^{-2} day^{-1})	Micro-graz (mg C m^{-2} day^{-1})	Meso-graz (mg C m^{-2} day^{-1})
Phytoplankton community				
TChl*a*_fluoro	1390 ± 133	990 ± 106	645 ± 62	349 ± 62
FCM_sum pop	1390 ± 133	862 ± 71	673 ± 62	231 ± 53
TChl*a*_40m_fluoro		930 ± 89	601 ± 61	
TChl*a*_40m_HPLC		767 ± 78	430 ± 62	
Major groups				
*Prochlorococcus*_fcm	157 ± 21	58 ± 14	54 ± 11	–
*Synechococcus*_fcm	392 ± 68	190 ± 29	236 ± 39	–
Pico-eukaryotes_fcm	230 ± 14	136 ± 14	115 ± 10	21 ± 15
Nano/microeuks_fcm	605 ± 72	478 ± 52	268 ± 34	210 ± 44
Diatoms/FUCO_HPLC	15 ± 3	31 ± 10	5 ± 2	26 ± 9
Prymnes/HEX_HPLC	103 ± 7	60 ± 13	34 ± 8	28 ± 13
Other AEuks_HPLC	722 ± 72	555 ± 126	233 ± 67	322 ± 80

Estimates are means ± standard error for 13 experimental profiles (Exp. 4–16, Table I) integrated to 80–100 m (full euphotic zone) or upper 40 m (HPLC, others as indicated). Biomass estimates are from microscopy and flow cytometry (Taylor *et al.*, 2015). Rate estimates are from *in situ* dilution incubations analyzed by flow cytometry (FCM) and pigments (fluorometry, HPLC) (Selph *et al.*, 2015). Mesozooplankton grazing estimates based on TChl*a* were determined independently for each experiment from measured phytoplankton biomass and gut pigment estimates of instantaneous grazing impact on phytoplankton (Table I). Mesozooplankton grazing estimates from FCM are experimental differences between production and micrograzing on eukaryotic phytoplankton, assuming that growth and grazing are in balance. Growth–grazing balance is also assumed for group-specific estimates for mesozooplankton grazing from HPLC pigments.

measurements by HPLC are ~18% lower than that from shipboard fluorometry. However, the rate differences between production and microzooplankton grazing from both TChl*a* analyses yield comparable estimates for mesozooplankton grazing (329–349 mg C m^{-2} day^{-1}). In contrast, assuming a growth–grazing balance for FCM-based populations leads to lower absolute and relative rates of mesozooplankton grazing (231 ± 53 mg C m^{-2} day^{-1} and 27 versus 36% of production, respectively) than the pigment-based results.

Among the major groups examined, the picophytoplankton populations (PRO, SYN, P-Euks) contribute disproportionately less to community productivity than to biomass (39 versus 56%, respectively), whereas diatoms contribute disproportionately more, though still a very small proportion of the total (3–4 versus 1%) (Table II). Other categories are more similar in biomass and production contributions, given uncertainties in the rate assessments. Despite their small contribution to community production, diatoms are as important in the bulk diet of mesozooplankton as production by picophytoplankton or prymnesiophytes (which are also partially included in the pico-size class; Taylor *et al.*, 2015). In contrast, except for the small surplus for picoeukaryotes, the production of picophytoplankton is fully accounted for by microzooplankton grazing, with SYN grazing exceeding production estimates. Picophytoplankton comprise the major dietary flux to microherbivores (405 mg C m^{-2} day^{-1}), roughly 60% of the total, whereas larger eukaryotes (268 mg C m^{-2} day^{-1}) support the remaining 40%. More broadly, the sum of individual population components reasonably supports the full community estimates. For example, the pigment-based rate estimates for eukaryotes (Diatom, Prymnes, Other) plus FCM determinations for PRO and SYN (sums = 894, 562 and 376 mg C m^{-2} day^{-1} for production, micro- and mesozooplankton herbivory, respectively) agree roughly with the magnitudes of total community rates. While there are modest differences in these rate comparisons, which may reflect the different parameters measured and different depths of rate integration, there is little that stands out as glaring omissions or gross over- or underestimates.

DISCUSSION

Methodological considerations

The physical/chemical environment of the CRD is characterized by a shallow thermocline and very sharp gradients in temperature, nutrients and dissolved oxygen in the euphotic zone (Fiedler and Talley, 2006). Within the upper 40 m of the highest biological activity in our experiments, temperatures declined 11–12°C relative to surface values and oxygen concentrations decreased by an order of magnitude (Selph *et al.*, 2015). While oxygen variability is not believed to have influenced rate estimates in our incubations, temperature and light conditions at depth would have been difficult to reproduce in shipboard incubators. Our *in situ* incubation approach thus minimizes concern about errors due to unnatural incubation conditions. Occasional full dilution experiments conducted with mixed-layer seawater during the cruise also confirmed strong linear relationships between dilution and the net growth response of phytoplankton (Selph *et al.*, 2015). Systematic errors due to nonlinear dynamics are therefore unlikely.

The most satisfying population variables in our experiments were FCM assessments of picophytoplankton. Except for PRO, these analyses were done live on shipboard, and the raw abundance counts allowed for relatively unambiguous calculations of net rates of change for defined populations. Rate estimates for other variables require more careful interpretation. For pigment-based rates, for example, we reduced raw pigment growth rate estimates by the mean increase in red fluorescence per cell (cellular Chl*a* content) measured in initial and final FCM-analyzed samples. This correction is typical and necessary for experiments conducted in trace-metal limited waters, where phytoplankton pigment content responds more quickly than biomass growth to trace contaminants (Sanderson *et al.*, 1995; Landry *et al.*, 2003, 2011b). In this case, the applied subtraction for upper 20-m experiments averaged 0.46 day^{-1}, but dropped off quickly to negligible correction in deeper incubations. The near-surface factor is substantial enough, however, that uncorrected growth rate estimates would have easily matched the magnitude of ^{14}C estimates of phytoplankton production at shallow depths (Fig. 2), as well as resolved the apparent deficit of production to grazing in Table I. Thus, one methodological uncertainty is the possible underestimation of pigment-based production rates. Since our estimates already exceed mean historical field-measured rates of production for the CRD region by almost a factor of 3, we take some reassurance from the fact that they are conservative. Nonetheless, correcting all pigment growth rates for all experiments by the same mean depth-dependent factors has implications for the calculations and comparisons of pigment-based rates for individual populations. These unfortunately could not be resolved further in the present analysis.

If our TChl*a*-based production estimates of ~1 g C $m^{-2}$$day^{-1}$ are conservative underestimates, then the discrepancy between community rates based on TChl*a* and FCM analyses could increase (Table II). While FCM analyses seem to capture well the dynamics of well-defined picoplankton populations, the TChl*a* rates, even with

correction uncertainty, provide a better index of biomass production than the full community assessment derived from FCM populations. The FCM problem is principally with the diverse assemblage of larger eukaryotic cells, whose biomass changes cannot be reliably determined from cell counts. Despite this, we note that the combined production estimates for all eukaryotic phytoplankton are not that much different between FCM and pigment-based approaches (614 versus 646 g C m^{-2} day^{-1}, respectively; Table II). Unless these independent determinations are both incorrect by about the same amount and in the same direction, we take this agreement as reasonable indication that we have converged on realistic production estimates for the community.

As noted previously, Table I raises the prospect that instantaneous grazing rates of mesozooplankton could be overestimated by contamination of gut analysis samples by phaeopigment-containing detritus. Given the net growth–grazing discrepancy in Table I, an average contamination factor of ~40% of the phaeopigment values resolves this difference in the absence of other corrections, such as possible underestimation of production discussed above. Inspection of Table I reveals, however, some very high values (e.g. Exps. 10 and 18) that account for most of the difference between instantaneous growth and grazing rates, suggesting that the majority of results are reasonable. In addition, the carbon-based estimate of mesozooplankton grazing derived from uncorrected gut pigment results in Table II closely matches the surplus phytoplankton production determined from TChl*a* analyses of the dilution incubations (i.e. the difference between phytoplankton growth and microzooplankton grazing). Tables I and II seem nonetheless to support contrasting conclusions about a strong production–grazing balance in the CRD.

The obvious difference between Tables I and II is that results from Exps. 1–3 and 17–19 were excluded from the latter because they lacked data on phytoplankton carbon biomass (resources were insufficient for microscope analyses of these experiments). By circumstance, these excluded experiments all have negative net growth–grazing balances in Table I. Even without these experiments, however, there is still a substantial net growth rate deficit (0.16 day^{-1}) in Table I for Exps. 4–16. The effect on Table II is mainly reduced because large instantaneous rate estimates (like 1.82 day^{-1} for Exp. 10) have less impact when computed in terms of the carbon consumed. For the purposes of the following discussion, we suggest that instantaneous rate estimates of mesozooplankton grazing (Table I) could be inflated in some cases by contamination, but these overestimates do not dominate the carbon-based grazing average (Table II), which supports a general production–grazing balance for the region.

Phytoplankton production and fate in the CRD

The international EASTTROPAC expedition in 1967–1968, a major field program of its day, provided the first seasonal surveys of the eastern topical Pacific, resulting in numerous publications as well as Atlas maps of the regional physical, chemical and biological oceanography (Love, 1972–1978). The US National Marine Fisheries Service continues to conduct major ETP surveys periodically, with emphasis on higher trophic levels, notably marine mammals, turtles and seabirds and their epi- and mesopelagic prey (Fiedler, 2002; Vilchis *et al.*, 2006, 2009). For the CRD specifically, however, individual projects and cruises have mainly led the way in exploring and highlighting the area's unique planktology, such as the very high abundances of picophytoplankton (Li *et al.*, 1983; Saito *et al.*, 2005) and the physiological and ecological adaptations of microbes and animal inhabitants to the strong, shallow oxygen minimum zone, the global ocean's largest, that underlies the region. Surprisingly however, there have been few studies focusing on euphotic zone productivity and trophic interactions in the CRD. To our knowledge, there are no community assessments of zooplankton community grazing for the CRD, and there is only one microzooplankton study (Olson and Daly, 2013), with one experimental dilution incubation with central CRD surface water that found microzooplankton grazing in slight excess of phytoplankton growth at that location. Early production estimates from EASTROPAC (Owen and Zeitzschel, 1970) put the CRD vicinity, ~200–400 mg C m^{-2} day^{-1}, slightly higher than the seasonal range for the region (130–320 mg C m^{-2} day^{-1}). However, these values are considered to be underestimates of actual production rates (Banse and Young, 1990), as are most from that era. Nonetheless, more modern shipboard production estimates for the Papagayo subregion, which includes the CRD, are not much higher (365 mg C m^{-2} day^{-1}; Pennington *et al.*, 2006).

Despite the paucity of experimentally based production and grazing measurements for the CRD, the present results are well anticipated by insights and inferences from historical studies. For example, from patterns observed for phytoplankton–zooplankton depth relationships in EASTROPAC sampling, Longhurst (Longhurst, 1976) hypothesized that phytoplankton distributions in the stable tropical oceans were regulated by zooplankton grazing pressure, rather than by sinking as generally assumed at the time, with highest grazing aligning with the depth strata of highest productivity. Similarly, well before the importance of microbial food webs in marine systems was broadly appreciated, Beers and Stewart

(Beers and Stewart, 1971) inferred from EASTROPAC measurements of microzooplankton biomass that microherbivores could consume the majority (70%) of regional primary production and impact such open-ocean habitats more than coastal ecosystems. Such thinking now represents a generally accepted paradigm for phyto–zooplankton production dynamics in tropical and subtropical waters, supported broadly by field-measured rates (Landry *et al.*, 1997; Calbet and Landry, 2004). Nonetheless, historical primary production values for the CRD area have been flagged as unrealistically low relative to those suggested by models. Pennington *et al.* (Pennington *et al.*, 2006) indicate, for example, that the vertically generalized productivity model, based on sea surface temperature, irradiance and satellite chlorophyll data (Behrenfeld and Falkowski, 1997), gives production values of 997 mg C m^{-2} day^{-1} for the Papagayo subregion, approximately three times higher than ship-based measurements.

The present study brings these various insights and speculations together into one coherent production–grazing analysis based on rigorous process-rate field measurements. From this analysis, we can see that the CRD supports relatively high productivity of ~1 g C m^{-2} day^{-1}, that this production is partitioned by relatively tight grazing coupling of about 2/3 to microzooplankton and 1/3 to mesozooplankton and that picophytoplankton play a major role in system productivity. Picophytoplankton production is almost entirely consumed by microherbivores, whereas larger phytoplankton are mainly grazed by larger zooplankton in the upper euphotic zone (as hypothesized by Longhurst, 1976). We view the actual rate estimates from this analysis as conservative for the region in summer, typically the season of strongest dome development, based on the methodological considerations discussed above and the fact that 2010 was a moderate El Niño year. Satellite imagery showed weak signals in surface temperature and chlorophyll during our cruise, compared with what is normally the case in July (Landry *et al.*, this issue). In addition, population abundances of *Synechococcus* were notably an order of magnitude lower than maximal values observed on previous cruises (Li *et al.*, 1983; Saito *et al.*, 2005). These differences suggest that higher production rates, higher picophytoplankton biomass and perhaps substantial differences in community composition, distributions and grazing relationships could occur during normal or accelerated doming years. Of particular relevance to our analysis, one might expect a sharper contrast during normal years between production–grazing dynamics in the vicinity of the dome center relative to the regional average and adjacent waters. However, given a possible 10-fold increase in SYN biomass, it is not clear to what extent enhanced doming (or La Niña) conditions might alter the distribution of production between pico- and larger phytoplankton. Here, we averaged experiments (Exps. 4–7, 12–15) conducted in and out of the central dome region because the biomass, rates and relationships overall were not that different (Selph *et al.*, 2015; Taylor *et al.*, 2015). Sharper gradients and higher standing stocks associated with stronger doming in the central area could change this significantly.

In addition to uncertainty with regard to "normal" production rates and fates in the CRD, we found plankton stocks and processes to be substantially more variable than expected or encountered previously in the upwelling area of the eastern equatorial Pacific. In this extensive region between 4°N–4°S and 110–140°W and on two seasonal cruises, growth rate estimates from independent dilution experiments at different depths in the upper mixed layer varied within a few percent (Landry *et al.*, 2011a) and standing stocks and rate estimates varied typically within a factor of 2 or 3 (Selph *et al.*, 2011; Taylor *et al.*, 2011). We had hoped to do better than that in the CRD using a drogued drift array to stay in reasonable proximity to marked water parcels for day-to-day experimental sampling. Instead, even when sampling adjacent to the drifter, we found abrupt and unexplained changes in community composition (Taylor *et al.*, 2015), more than could be explained by measured process rates and clearly indicative of a strongly sheared and variable upper euphotic zone, despite the appearance of relative chlorophyll constancy. While we dealt with this variability pragmatically, by averaging experiments, investigating how such system variability relates to diversity maintenance of microbial populations based on fine-scale sampling and appropriate molecular methods would be an interesting topic for future investigation.

The apparent overgrazing of SYN by microzooplankton in our experiments is another finding with potentially interesting implications for future study in the CRD. This result occurs to greater or lesser extent in 13 of 18 rate profiles. It is therefore not dominated by one or two very high values, but instead seems to be a general system characteristic. In addition, there is clear mesozooplankton grazing on SYN, including our own observations of visible SYN in zooplankton fecal pellets as well as suggestions that this is the main route by which the cells find their way into sediment traps below the euphotic zone (Stukel *et al.*, 2013). Since our grazing estimates for SYN must be conservative by including only consumption by microzooplankton, it is possible that their growth rate has been underestimated by leaving out a critical part of their growth environment, hypothetically, the environment internal to mesozooplankton guts, discarded fecal pellets and, ultimately, the aggregates that form from disintegrating pellets, which would appear to be the fate of most of the egesta produced by CRD mesozooplankton (Stukel *et al.*,

2013). It is known, for example, that SYN can pass through mesozooplankton guts intact (Silver and Bruland, 1981; Johnson *et al.*, 1982; Gorsky *et al.*, 1999). The question is whether the cells benefit sufficiently from the relative nutritional richness of those microhabitats to account for at least a 24% increase in their production rates, the mean offset between measured production and microzooplankton grazing losses in our experiments, and then re-enter the microbial food web as prey for protistan consumers.

Comparisons of ETP production centers

The CRD clearly differs in production magnitude and community composition from the major high productivity area of the ETP, the Peruvian coastal upwelling system. Production rates averaged over the broad area influenced by the Peru upwelling (3580 and 2087 mg C m^{-2} day^{-1} according to mean ship and model values, respectively; Pennington *et al.*, 2006) are two to four times high than our estimates for the CRD. In addition, large diatoms dominate that system, which facilitates efficient transfer to higher trophic levels, including direct feeding on diatom blooms by the dominant pelagic fish, anchoveta (*Engraulis ringens*).

In contrast, based on results from similar process-rate studies, the CRD compares favorably with the eastern equatorial upwelling region. From 31 full euphotic zone experiments conducted in equatorial waters between 4°N and 4°S, 110–140°W, community phytoplankton biomass (1385 ± 93 mg C m^{-2}) and phytoplankton production (867 ± 96 mg C m^{-2} day^{-1}) are very similar to estimates from the present study (Table II), as are a general balance between production and grazing processes and the approximate 2/3 and 1/3 splits between micro- and mesozooplankton herbivory (Landry *et al.*, 2011a). As in the CRD, grazing by microconsumers in the equatorial Pacific largely accounts for the production of picophytoplankton. Several substantial differences are, however, evident in the details. The euphotic zone in the equatorial upwelling region is about double the depth of the CRD and generally lacks the shallow subsurface peak observed in CRD Chl*a* profiles. Measured ^{14}C-primary production rates were notably higher by ~50% during the period of our study in the CRD than in the equatorial region (1025 ± 113 versus 672 ± 73 mg C m^{-2} day^{-1}), suggesting potentially missing contributions to production in the CRD flux analysis, or possible methodological explanations for the ^{14}C-uptake differences (the equatorial samples were from a trace-metal clean rosette; Balch *et al.*, 2011). More strikingly, the equatorial region showed much higher biomass and production rates for diatoms (7 and 18% of the community totals, respectively), despite the somewhat lower overall productivity. Conversely, the picophytoplankton, dominated by PRO, in the equatorial region contributed less to total community biomass and production (40 and 27%, respectively) than the SYN-dominated picophytoplankton in the CRD (56 and 39%, respectively), although the relative decreases from biomass to production contributions are similar. That the CRD seems to select for a community composition with a much lower proportion of diatoms to picophytoplankton seems incongruous with its marginally higher system richness and its proximity to seasonal influence and seeding from diatom blooms off coastal Central America. The present analysis provides no easy explanation for these differences in terms of trophic coupling or partitioning ratios between micro- and mesozooplankton consumers. If anything, the greater prevalence of gelatinous consumers in the CRD, notably pelagic tunicates (appendicularians, salps, doliolids and pyrosomes) that are functionally capable of feeding directly on small phytoplankton cells (Décima *et al.*, 2015), would seem to be selected for by the increased importance of smaller prey in the CRD, as opposed to their presence being a significant factor for why that occurs.

ACKNOWLEDGEMENTS

We thank the captain, crew and research technicians of the R/V Melville, whose efforts contributed significantly to the success of our cruise. We also gratefully acknowledge Daniel Wick, Kate Tsyrklevich, Darcy Taniguchi, Alain de Verneil, Kelly Keebler and Alison Brandeis for their help with the shipboard experiments and sample processing.

FUNDING

This component of the CRD FLUZiE study was supported by U.S. National Science Foundation grant OCE-0826626 to M.R.L. Additional support was provided by a Ramón Areces Foundation Fellowship to A.G.R., a NASA National Aeronautics and Space Administration, Earth and Space Science Fellowship to M.R.S. and a National Science Foundation Graduate Research Fellowship to A.L.P.

REFERENCES

Balch, W. M., Poulton, A., Drapeau, D. T., Bowler, B. C., Windecker, L. A. and Booth, E. S. (2011) Zonal and meridional patterns of phytoplankton biomass and carbon fixation in the Equatorial Pacific Ocean, between 110°W and 140°W. *Deep Sea Res. II*, **58**, 400–416.

Banse, K. and Young, M. (1990) Sources of variability in satellite-derived estimates of phytoplankton production in the Eastern Tropical Pacific. *J. Geophys. Res.*, **95**, 7201–7215.

Beers, J. R. and Stewart, G. L. (1971) Micro-zooplankters in the plankton communities of the upper waters of the eastern tropical Pacific. *Deep Sea Res.*, **18**, 861–883.

Behrenfeld, M. J. and Falkowski, P. G. (1997) Photosynthetic rates derived from satellite-based chlorophyll concentration. *Limnol. Oceanogr.*, **42**, 1–20.

Binder, B. J., Chisholm, S. W., Olson, R. J., Frankel, S. I. and Worden, A. Z. (1996) Dynamics of picophytoplankton, ultraphytoplankton and bacteria in the central equatorial Pacific. *Deep Sea Res. II*, **43**, 907–931.

Brown, S. L., Landry, M. R., Selph, K. E., Yang, E. J., Rii, Y. M. and Bidigare, R. R. (2008) Diatoms in the desert; plankton community response to a mesoscale eddy in the subtropical North Pacific. *Deep Sea Res. II*, **55**, 1321–1333.

Calbet, A. and Landry, M. R. (2004) Phytoplankton growth, microzooplankton grazing and carbon cycling in marine systems. *Limnol. Oceanogr.*, **49**, 51–57.

Chavez, F. P., Buck, K. R., Service, S. K., Newton, J. and Barber, R. T. (1996) Phytoplankton variability in the central and eastern tropical Pacific. *Deep Sea Res. II*, **43**, 835–870.

Décima, M., Landry, M. R. and Rykaczewski, R. (2011) Broad-scale patterns in mesozooplankton biomass and grazing in the Eastern Equatorial Pacific. *Deep Sea Res. II*, **58**, 387–399.

Décima, M., Landry, M. R., Stukel, M. R., López-López, L. and Krause, J. W. (2015) Mesozooplankton biomass and grazing in the Costa Rica Dome: amplifying variability through the plankton food web. *J. Plankton Res.*, in press.

Durbin, E. G. and Campbell, R. G. (2007) Reassessment of the gut pigment method for estimating *in situ* zooplankton ingestion. *Mar. Ecol. Prog. Ser.*, **331**, 305–307.

Fiedler, P. C. (2002) The annual cycle and biological effects of the Costa Rica Dome. *Deep Sea Res. I*, **49**, 321–338.

Fiedler, P. C. and Talley, L. D. (2006) Hydrography of the eastern tropical Pacific: a review. *Progr. Oceanogr.*, **69**, 143–180.

Garrison, D. L., Gowing, M. M., Hughes, M. P., Campbell, L., Caron, D. A., Dennett, M. R., Shalapyonok, A., Olson, R. J. *et al.* (2000) Microbial food web structure in the Arabian Sea: a US JGOFS study. *Deep Sea Res. II*, **47**, 1387–1422.

Goericke, R. (2002) Top-down control of phytoplankton biomass and community structure in the monsoonal Arabian Sea. *Limnol. Oceanogr.*, **47**, 1307–1323.

Gorsky, G., Chretiennot-Dinet, M. J., Blanchot, J. and Palazzoli, I. (1999) Picoplankton and nanoplankton aggregation by appendicularians: fecal pellet contents of *Megalocercus huxleyi* in the equatorial Pacific. *J. Geophys. Res. Oceans*, **104**, 3381–3390.

Johnson, P. W., Xu, H. S. and Sieburth, J. M. (1982) The utilization of chroococcoid cyanobacteria by marine protozooplankters but not by calanoid copepods. *Ann. Inst. Oceanogr.*, **58**, 297–308.

Kleppel, G. S. and Pieper, R. E. (1984) Phytoplankton pigments in the gut contents of planktonic copepods from coastal waters off Southern California. *Mar. Biol.*, **78**, 193–198.

Landry, M. R., Barber, R. T., Bidigare, R. R., Chai, F., Coale, K. H., Dam, H. G., Lewis, M. R., Lindley, S. T. *et al.* (1997) Iron and grazing constraints on primary production in the central equatorial Pacific: an EqPac synthesis. *Limnol. Oceanogr.*, **42**, 405–418.

Landry, M. E., Brown, S., Neveux, J., Dupouy, C., Blanchot, J., Christensen, S. and Bidigare, R. R. (2003) Phytoplankton growth and microzooplankton grazing in high-nutrient, low-chlorophyll waters of the equatorial Pacific: community and taxon-specific rate assessments from pigment and flow cytometric analyses. *J. Geophys. Res.*, **108**(C12), 8142.

Landry, M. R., Brown, S. L., Rii, Y. M., Selph, K. E., Bidigare, R. R., Yang, E. J. and Simmons, M. P. (2008) Depth-stratified phytoplankton dynamics in Cyclone *Opal*, a subtropical mesoscale eddy. *Deep Sea Res. II*, **55**, 1348–1359.

Landry, M. R., Constantinou, J., Latasa, M., Brown, S. L., Bidigare, R. R. and Ondrusek, M. E. (2000) Biological response to iron fertilization in the eastern equatorial Pacific (IronEx II). III. Dynamics of phytoplankton growth and microzooplankton grazing. *Mar. Ecol. Prog. Ser.*, **201**, 57–72.

Landry, M. R., De Verneil, A., Goes, J. I. and Moffett, J. W. (this issue) Plankton dynamics and biogeochemical fluxes in the Costa Rica Dome: introduction to the CRD flux and zinc experiments. *J. Plankton Res.*, in review.

Landry, M. R., Ohman, M. D., Goericke, R., Stukel, M. R. and Tsyrkevich, K. (2009) Lagrangian studies of phytoplankton growth and grazing relationships in a coastal upwelling ecosystem off Southern California. *Prog. Oceanogr.*, **83**, 208–216.

Landry, M. R., Selph, K. E., Taylor, A. G., Décima, M., Balch, W. M. and Bidigare, R. R. (2011a) Phytoplankton growth, grazing and production balances in the HNLC equatorial Pacific. *Deep Sea Res. II*, **58**, 524–535.

Landry, M. R., Selph, K. E. and Yang, E.-J. (2011b) Decoupled phytoplankton growth and microzooplankton grazing in the deep euphotic zone of the HNLC equatorial Pacific. *Mar. Ecol. Prog. Ser.*, **421**, 13–24.

Li, W. K. W., Subba Rao, D. V., Harrison, W. G., Smith, J. C., Cullen, J. J., Irwin, B. and Platt, T. (1983) Autotrophic picoplankton in the tropical ocean. *Science*, **219**, 292–295.

Longhurst, A. R. (1976) Interactions between zooplankton and phytoplankton profiles in the eastern tropical Pacific Ocean. *Deep Sea Res.*, **23**, 729–754.

Love, C. M. (ed.) (1972–1978) *EASTROPAC Atlas*, vols. 1–11. National Marine Fisheries Service, Washington, DC.

Menden-Deuer, S. and Lessard, E. J. (2000) Carbon to volume relationships for dinoflagellates, diatoms and other protist plankton. *Limnol. Oceanogr.*, **45**, 569–579.

Monger, B. C. and Landry, M. R. (1993) Flow cytometric analysis of marine bacteria with Hoechst 33342. *Appl. Environ. Microbiol.*, **59**, 905–911.

Olson, M. B. and Daly, K. L. (2013) Micro-grazer biomass, composition and distribution across prey resource and dissolved oxygen gradients in the far eastern tropical North Pacific Ocean. *Deep Sea Res.*, **75**, 28–38.

Owen, R. W. and Zeitzschel, B. (1970) Phytoplankton production: seasonal change in the oceanic eastern tropical Pacific. *Mar. Biol.*, **7**, 32–36.

Pennington, J. T., Mahoney, K. L., Kuwahara, V. S., Kolber, D. D., Calienes, R. and Chavez, F. P. (2006) Primary production in the eastern tropical Pacific: a review. *Prog. Oceanogr.*, **69**, 285–317.

Saito, M. A., Rocap, G. and Moffett, J. W. (2005) Production of cobalt binding ligands in a *Synechococcus* feature at the Costa Rica upwelling dome. *Limnol. Oceanogr.*, **50**, 279–290.

Sanderson, M. P., Hunter, C. N., Fitzwater, S. E., Gordon, R. M. and Barber, R. T. (1995) Primary productivity and trace-metal contamination measurements from a clean rosette system versus ultra-clean Go-Flo bottles. *Deep Sea Res. II*, **42**, 431–440.

Selph, K. E., Landry, M. R., Taylor, A. G., Gutiérrez-Rodríguez, A., Stukel, M. R., Wokuluk, J. and Pasulka, A. (2015) Phytoplankton

production and taxon-specific growth rates in the Costa Rica Dome. *J. Plankton Res.*, doi:10.1093/plankt/fbv063.

Selph, K. E., Landry, M. R., Taylor, A. G., Yang, E. J., Measures, C. I., Yang, J. J., Stukel, M. R., Christensen, S. *et al.* (2011) Spatially-resolved taxon-specific phytoplankton production and grazing dynamics in relation to iron distributions in the Equatorial Pacific between 110 and 140°W. *Deep Sea Res. II*, **58**, 358–377.

Sherr, E. B. and Sherr, B. F. (1993) Preservation and storage of samples for enumeration of heterotrophic protists. In: Kemp, P. K. (ed.), *Handbook of Methods in Aquatic Microbial Ecology*. CRC Press, Boca Raton, pp. 207–212.

Silver, M. W. and Bruland, K. W. (1981) Differential feeding and fecal pellet composition of salps and pteropods, and the possible origin of the deep-water flora and olive-green cells. *Mar. Biol.*, **62**, 263–273.

Strickland, J. D. H. and Parsons, T. R. (1972) *A Practical Handbook of Seawater Analysis*. Fisheries Research Board, Ottawa, Canada.

Stukel, M. R., Décima, M., Selph, K. E., Taniguchi, D. A. A. and Landry, M. R. (2013) The role of *Synechococcus* in vertical flux in the Costa Rica upwelling dome. *Prog. Oceanogr.*, **112–113**, 49–59.

Taylor, A. G., Landry, M. R., Freibott, A., Selph, K. E. and Gutiérrez-Rodríguez, A. (2015) Patterns of microbial community biomass, composition and HPLC diagnostic pigments in the Costa Rica upwelling dome. *J. Plankton Res.*, in press.

Taylor, A. G., Landry, M. R., Selph, K. E. and Yang, E. J. (2011) Biomass, size structure and depth distributions of the microbial community in the eastern equatorial Pacific. *Deep Sea Res. II*, **58**, 342–357.

Vilchis, L. I., Ballance, L. T. and Fiedler, P. C. (2006) Pelagic habitat of seabirds in the eastern tropical Pacific: effects of foraging ecology on habitat selection. *Mar. Ecol. Prog. Ser.*, **315**, 279–292.

Vilchis, L. I., Ballance, L. T. and Watson, W. (2009) Temporal variability of neustonic ichthyoplankton assemblages of the eastern Pacific warm pool: can community structure be linked to climate variability? *Deep Sea Res. I*, **56**, 125–140.

Zhang, X., Dam, H. G., White, J. R. and Roman, M. R. (1995) Latitudinal variations in mesozooplankton grazing and metabolism in the central tropical Pacific during the US JGOFS EqPac Study. *Deep-Sea Res. II*, **42**, 695–714.